Reflection Spectrum of the Single Crystal of Wurster's Blue Perchlorate

Yasushi IYECHIKA, Kyuya YAKUSHI, and Haruo KURODA*

Department of Chemistry, Faculty of Science, The University of Tokyo, Hongo, Bunkyo-ku, Tokyo 113

(Received July 9, 1979)

The visible and near-infrared reflection spectrum of the single crystal of Wurster's blue perchlorate was measured at various temperatures over the range of 30—300 K, by using the microspectrophotometric method. The absorption spectra were derived by Kramers-Kronig transformation of the reflection spectra. The intensity ratio of the (0-0) and (0-1) vibronic bands of the local-excitation associated with the π-π^* ($^2B_{1u} \leftarrow {}^2B_{2g}$) transition of $TMPD^+$ was found to be anomalous when the spectrum was measured with the light polarized parallel to the b-axis, while not in the spectrum polarized parallel to the a-axis. The Davydov splitting between B_{3u} and B_{2u} components of this absorption band was found to be about 400 cm^{-1}. In the antiferromagnetic (low temperature) phase below 190 K, the charge-transfer band appeared in the a-axis spectrum, showing its absorption maximum at 11.6×10^3 cm^{-1}, and its intensity increased on lowering the temperature. At the same time, a marked temperature dependence was observed in the local-excitation band. These changes are interpreted in terms of the singlet-triplet model of the dimeric interaction of $TMPD^+$ ions in the low-temperature phase.

N,N,N',N'-Tetramethyl-*p*-phenylenediamine perchlorate (Wurster's blue perchlorate, WBP) is a well-known example of stable cation radical salts, of which magnetic behaviors have been extensively studied.[1-8] This salt exhibits a phase transition between the paramagnetic (high-temperature) phase and the antiferromagnetic (low-temperature) phase, the specific heat peak corresponding to this phase transition having been observed at 189.9 K.[9] The temperature dependence of the spin susceptibility in the low-temperature phase was interpreted in terms of the singlet-triplet model assuming a dimeric interaction of the cation radical of *N,N,N',N'*-tetramethyl-*p*-phenylenediamine (TMPD).[3] This model was also shown to be consistent with the change of the absorption spectrum of WBP powder at low temperatures.[8,10] The dimeric arrangement of $TMPD^+$ ions was confirmed later by de Boer and Vos from the crystal structure analysis of the low-temperature phase of WBP.[11]

The optical properties of WBP crystal have been previously studied by several authors.[8,10,12-15] The polarized absorption spectrum of WBP crystal at room temperature was observed some years ago by Sakata and Nagakura[8] and by Tanaka and Mizuno,[13] both by employing a microspectrophotometric method for the observation of transmission spectrum. The polarized absorption spectrum of the low-temperature phase and its temperature dependence were studied in our laboratory also by use of a microspectrophotometer for transmission spectroscopy of small single crystal.[15] Although several important aspects have been revealed by those studies, the absorption spectra which were reported in these works, are not very satisfactory in the following respects: First, the resolutions of the spectra were not high enough to reveal the details of absorption bands, and, second, there remained some ambiguities as regards the crystallographic characters of the crystal faces on which the observations were carried out. The reflection spectrum of a crystal offers informations complementary to those obtainable from the absorption spectrum observed by transmission method, and, furthermore, in the case of a strongly-absorbing crystal like WBP, the reflection spectroscopy has several experimental advantages over the observation of transmission spectrum. The preliminary study of the reflection spectrum of WBP at low temperatures was carried out earlier by Anderson,[14] who made the observation on a mosaic arrangement of needle crystals of WBP without making any attempt to identify the crystallographic characters of the observing crystal faces.

In the present study, we constructed an apparatus to measure the polarized reflection spectrum of a single crystal of microscopic size at low temperatures, incorporating a cryostat with a microspectrophotometer for reflection spectroscopy. Using this apparatus, we have studied the polarized reflection spectrum of WBP crystal and its temperature dependence over the temperature range of 30—300 K.

Experimental

Material. WBP was prepared according to the method reported by Michaelis and Granick.[16] Small single crystals of WBP were grown by slowly cooling a hot methanol solution of WBP. The crystals thus obtained were either a needle having (011) crystal face, or a plate with the developed face of (001).

Microspectrophotometer and Cryostat. The reflection microspectrophotometer used in the present study, is the same as the one which was previously constructed and used by us to study the reflection spectrum of benzidine-TCNQ complex. The details of this apparatus were described in our previous paper.[17] The optical system of Olympus MMSP is used as the reflection microscope optical system of this apparatus. In order to carry out the measurement at low temperatures, we took off the rotatable sample stage of the microspectrophotometer and installed a cryostat as shown in the photograph of Fig. 1.

The main body of the cryostat is a cryogenic refrigerator, CTi SPECTRIM^{tm}, made by Cryogenic Technology Inc. It is horizontally supported on a specially designed stage with a mechanism to adjust its position in three directions X, Y, and Z, with an accuracy of 10 μ. At the cold head of the refrigerator, we installed the sample-holding device which is illustrated in Fig. 2. The sample crystal is fixed on a miniature goniometer head, so that we can adjust the crystal orientation with respect to the optical axis. The crystal is cooled by means of the heat conduction through the goniometer head and the copper block on which the former is fixed. The temperature is controlled by adjusting the current of the electric heater installed at the cold head, and measured with a Au(Fe)–chromel thermo-couple fixed at the goniometer head. For the purpose of the radiation

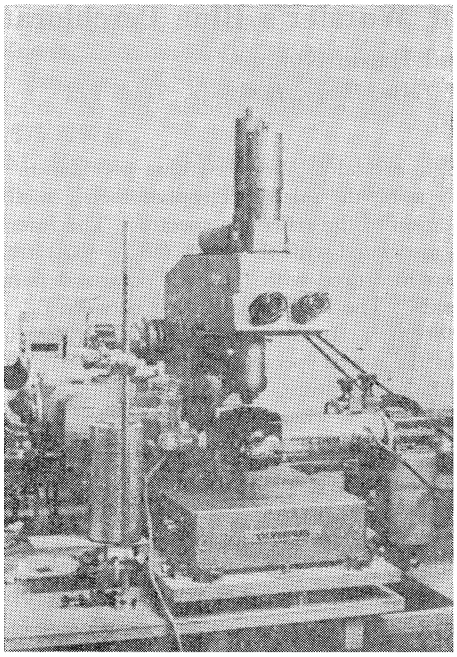

Fig. 1. Photograph of the microspectrophotometer with a low-temperature cryostat.

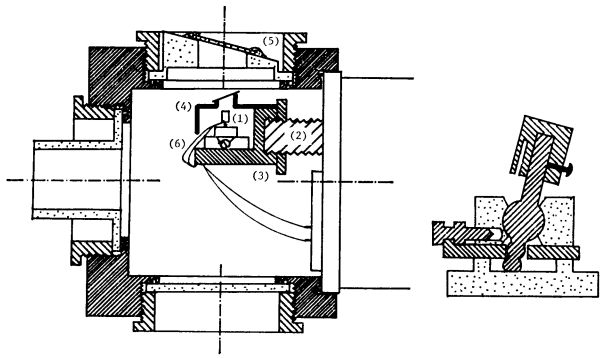

(a) (b)

Fig. 2. Schematic drawing of the sample-holding system: (a) Cross-section view of the sample chamber of the cryostat: (1) goniometer head, (2) cold head of the cryostat, (3) a copper block to support the goniometer, (4) a copper cup with a quartz window, (5) a quartz window, (6) thermo-couple.
(b) Structure of the miniature goniometer head.

shield and to avoid the water condensation on the crystal faces, we put a copper cup with a quartz window over the goniometer head. The face of the window is tilted from the horizontal plane by 30° to avoid the disturbance arising from the light reflection at the window. The system described above is covered with a vacuum-tight cover, and the inside of the above sample chamber was evacuated by the combined action of a rotary vacuum pump and a sorption pump. The pressure measured without the operation of the cryogenic refrigerator was about 5×10^{-5} Torr. Under the operation of the refrigerator, the pressure must be appreciably lower than the above value because of the cryogenic-pumping action of the cold head.

In the present study, we used an objective lens of the magnification of $\times5$. We had to use this lens of rather low magnification because of the requirement of a long working distance due to the geometry of our cryostat. The smallest size of the crystal face that can be used for the measurement of reflection spectrum, is 0.18 mmϕ under the condition adopted in the present study. The aperture angle of the used objective lens is 5.8°, so that we can safely treat the observed reflectance data as those obtained under the normal incidence condition.[18]

Analysis of Reflection Spectrum. Two different methods were employed in the present study to obtain optical constants from the measured reflectance data. The one was the dispersion analysis method (or curve-fitting method). In this case, we express the complex dielectric function as follows,

$$\varepsilon(\omega) = \varepsilon_c + \sum_j \frac{S_j\omega_j^2}{(\omega_j^2-\omega^2)-i\gamma_j\omega_j\omega} \tag{1}$$

and look for the parameter set, ε_c and $(\omega_j, \gamma_j, S_j)$, which gives the best agreement between the observed and calculated reflectance, using the following relation between the reflectance $R(\omega)$ and the complex dielectric function $\varepsilon(\omega)$.

$$R(\omega) = \frac{|\varepsilon(\omega)|+1-2\{|\varepsilon(\omega)|+\mathrm{Re}[\varepsilon(\omega)]\}^{1/2}}{|\varepsilon(\omega)|+1+2\{|\varepsilon(\omega)|+\mathrm{Re}[\varepsilon(\omega)]\}^{1/2}} \tag{2}$$

The optical constants, $n(\omega)$ and $k(\omega)$ of the crystal, can be obtained from $\varepsilon(\omega)$ by the following relations

$$\mathrm{Re}[\varepsilon(\omega)] = n(\omega)^2 - k(\omega)^2 \tag{3}$$

$$\mathrm{Im}[\varepsilon(\omega)] = 2n(\omega)k(\omega) \tag{4}$$

The details of the procedure of this analysis has been described in our previous paper.[17] The second method was the Kramers-Kronig analysis. To perform a direct Kramers-Kronig transformation, we need to know the reflectance over a very wide frequency range. However, our measurement of reflection spectrum was limited only in the near-infrared and visible region. Therefore, instead of carrying out a direct Kramers-Kronig transformation, we used the modified method which was proposed by Ahrenkiel.[21] This method was able to be successfully used in the present case. In order to see the spectrum corresponding to the absorption spectrum, we plotted the imaginary part of the complex dielectric constant, $\mathrm{Im}[\varepsilon(\omega)]$ against the frequency or wave number.

The method of obtaining the oscillator strength of an absorption band was as follows. In the case of dispersion analysis, we used one dispersion term.

$$\varepsilon[j](\omega) = S_j\omega_j^2/[(\omega_j^2-\omega^2) - i\gamma_j\omega_j\omega],$$

for each absorption bands.[19] Then the oscillator strength of the band (j) was calculated by the following equation.

$$f_{(j)} = \frac{m}{2\pi^2e^2N}\int_0^\infty \mathrm{Im}\,\varepsilon[j](\omega)\omega\,\mathrm{d}\omega,$$

where N is the number density of electrons concerned with the j-th transition, m is the electron mass, and e is the electron charge.

In the case of Kramers-Kronig analysis, the oscillator strength was calculated as follows,

$$f_{(j)} = \frac{m}{2\pi^2e^2N}\int_{\omega_a}^{\omega_b}\varepsilon_2(\omega)\omega\mathrm{d}\omega$$

where ω_a and ω_b are the low- and high-wave number limits of the concerned band. When absorption bands are overlapping on each other, there remains some arbitrariness as regards their decomposition. This gives a slight uncertainty of the oscillator-strengths of decomposed bands.

Results and Discussion

Spectrum at Room Temperature. The crystal of

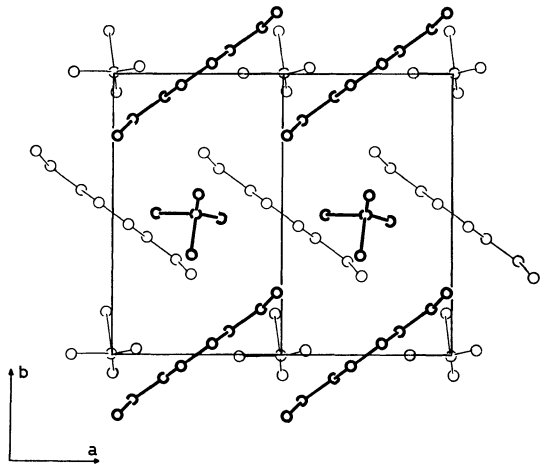

Fig. 3. Projection of the crystal structure of the high-temperature phase of WBP onto the (001) plane.

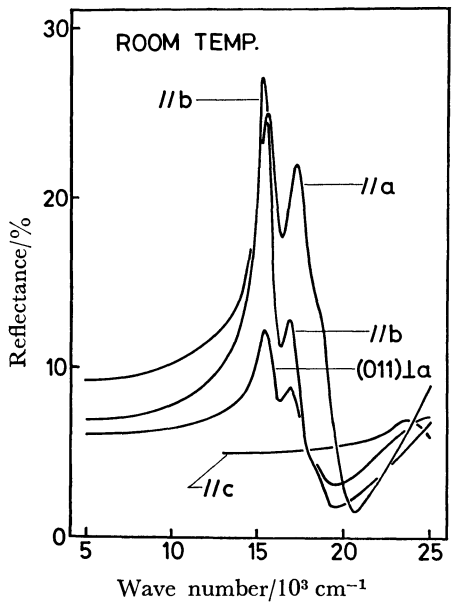

Fig. 4. Room-temperature reflection spectra observed on the (001), (011) and (010) crystal faces.

WBP is orthorhombic with the space group Pnnm, and the lattice constants, $a=5.956$ Å, $b=10.229$ Å, and $c=10.187$ Å.[11] Two molecular units of $TMPD^{+}\cdot ClO_4^{-}$, which are mutually related by the symmetry operation of a glide plane, are contained in the unit cell. The projection of the crystal structure, reported by de Boer and Vos,[11] is reproduced in Fig. 3.

Figure 4 shows the reflection spectra measured on the (001) face for the //a and //b polarizations and those measured on the (011) face for the //a and ⊥a polarizations. A prominent dispersion of reflectance appears in the region of 13×10^3—20×10^3 cm^{-1}. This is the region where the absorption band due to the lowest π-π^* transition ($^2B_{1u}\leftarrow{}^2B_{2g}$) of $TMPD^{+}$ ion appears in the solution spectrum of WBP. The polarization direction which gives the strongest dispersion, agrees with the one that is expected for the local excitation band associated with the $^2B_{1u}\leftarrow{}^2B_{2g}$ transition which has its transition moment parallel to the long molecular axis. Below 14×10^3 cm^{-1}, the observed

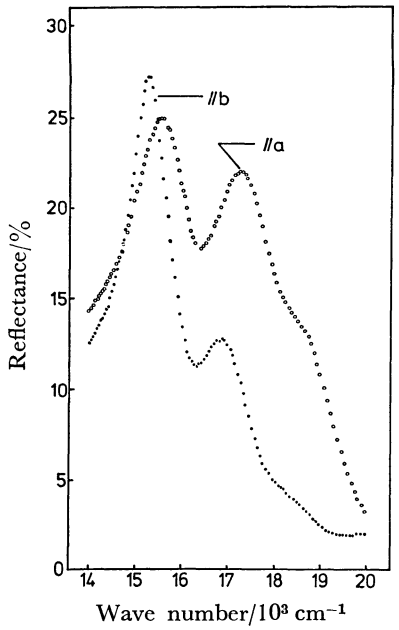

Fig. 5. Reflection spectra measured with 1.6 nm resolution at room temperature.

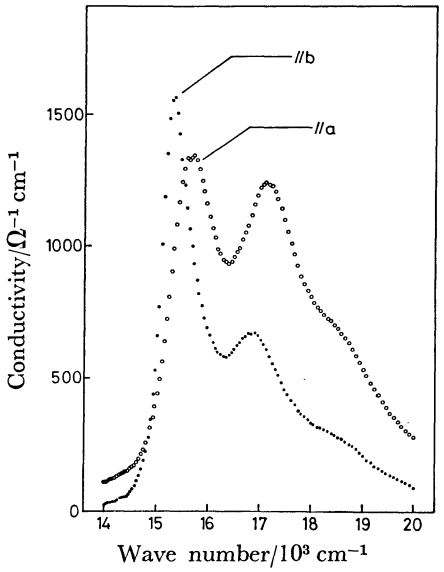

Fig. 6. Optical conductivity spectra obtained by the Kramers-Kronig transformation of the reflection spectra shown in Fig. 5.

reflection spectra show no distinct dispersion except a slight indication of the presence of a shoulder on the low-wave number tail of the //a spectrum of the (011) face, although a dispersion clearly appears around 11×10^3 cm^{-1} in the //a reflection spectrum observed at low temperatures as we will show later. The shape of the //a reflection spectrum which was reported by Anderson,[14] resembles to our //a spectrum of the (011) face, but the reflectance values reported by him, are significantly lower as compared with those obtained in the present study. This is naturally expected since his data were obtained on a mosaic arrangement of needle crystals, not on a good single crystal.

In order to reveal the details of the structure ap-

TABLE 1. OBSERVED WAVE NUMBERS AND OSCILLATOR STRENGTHS OF THE VIBRONIC BANDS IN THE LE BAND OF THE SPECTRUM OF WBP

Polarization direction	$\cos^2\theta$[a]	(0-0)band		(0-1)band		(0-2)band		f_t[b]
		$\bar{\nu}_{max}/cm^{-1}$	f	$\bar{\nu}_{max}/cm^{-1}$	f	$\bar{\nu}_{max}/cm^{-1}$	f	
// a	0.643	15800	0.24	17380	0.24	shoulder	≈0.1	0.61
// b	0.357	15430	0.19	16980	0.13	shoulder	≈0.05	0.38
// c	0.000	—	0.00	—	0.00	—	0.00	0.00
		($\Delta\bar{\nu}$[c]) = 370 cm^{-1}		400 cm^{-1}		—)		
Solution		16300	0.05	17700	0.06	shoulder	≈0.03	0.16

a) Squares of the direction cosines of the long axis of $TMPD^+$ ion to the crystallographic axes. b) Total oscillator strength. c) Splitting between the //a and //b bands ($\Delta\bar{\nu}=\bar{\nu}_{max}(//a)-\bar{\nu}_{max}(//b)$).

pearing in the reflection spectrum, we carried out the measurement with an increased resolution over the region from 14×10^3 cm^{-1} to 20×10^3 cm^{-1} [20]. The results are shown in Fig. 5. Figure 6 shows the optical conductivity spectra† which were obtained by the Kramers-Kronig transformation of the reflectance data given in Fig. 5. As we have already mentioned, the absorption band appearing here can be safely attributed to the local excitation (LE) associated with the $^2B_{1u}\leftarrow{}^2B_{2g}$ transition of $TMPD^+$. The obtained optical conductivity spectra resemble to the solution spectrum of $TMPD^+$ ion, having the vibrational progression of about 1530 cm^{-1} which can be attributed to an intramolecular vibration of $TMPD^+$. We decomposed the observed absorption band into vibronic bands, and estimated the oscillator strength of each vibronic band. The results are given in Table 1, together with the corresponding values of the solution spectrum. In Table 1, we give also the total oscillator strength f_t and the square of the direction cosines of the long molecular axis of $TMPD^+$ with respect to the a- and b-axes. The ratio of the observed oscillator strengths, $f_t(//b)/f_t(//a)=0.63$, is in good agreement with the value, 0.56, that is expected on the basis of the oriented-gas model. This is in accord with what one can expect for a LE band due to a strong, long-axis polarized transition of $TMPD^+$ ion. In the case of this absorption band, a deviation of the oscillator-strength ratio $f_t(//b)/f_t(//a)$ from the oriented-gas value, could arise either from the crystal-induced mixing of some intramolecular transition which are polarized perpendicular to the long molecular axis, or from the mixing of an intermolecular charge-transfer (CT) transition. However, in WBP crystal, the mixing of a short-axis polarized transition of $TMPD^+$ with a long-axis polarized transition is forbidden by the site symmetry of $TMPD^+$. Although the n-π^* transition of $TMPD^+$ and the intermolecular CT transition between $TMPD^+$ ions could mix with the long-axis polarized transition of $TMPD^+$, the mixings of these transitions can not significantly affect the polarization ratio of the above LE band, because the oscillator strengths of the n-π^* and CT transitions are quite small in the present case.[22] As for the absolute value of oscillator strength, we note that the values determined from the //a and //b spectra of WBP crystal are about twice the oriented-gas values calculated by use of the oscillator strength of the $^2B_{1u}\leftarrow{}^2B_{2g}$ band of the solution spectrum of $TMPD^+$ ion.[23] Seemingly, this fact indicates that the oscillator strength of the above LE band has been significantly enhanced in WBP crystal. This enhancement of oscillator strength is likely to be due to the crystal-induced mixing of higher-energy, long-axis polarized, strong transitions of $TMPD^+$.

The most interesting aspect that can be noted in Fig. 6 (or in Table 1), is that the intensity ratio of the (0-0) and (0-1) vibronic bands is significantly different between the //a and //b optical conductivity spectra. The band shape in the //b spectrum is very much different from that of the solution spectrum, while the band shape in the //a spectrum resembles to the solution spectrum. In the //b spectrum, the (0-0) vibronic band is appreciably sharper and its intensity relative to the (0-1) vibronic band is significantly higher as compared with the solution spectrum. This phenomenon is similar to the *J*-band of the helix polymer of the pseudo-isocyanine dye, where the (0-0) band becomes sharp and markedly strong as compared with other vibronic bands when the spectrum is observed with the light polarized parallel to the direction of the helix.[24] This characteristic feature of *J*-band has been explained in terms of the collective excitation along the chain. A possible explanation for the shape of the LE band of WBP can be given from the consideration of the exciton-phonon coupling and the exciton band width. The shape of an absorption band of a molecular crystal was theoretically discussed by Sumi,[25] who showed by the model calculation that the intensity of an absorption band will be more and more concentrated into its (0-0) band on increasing the strength of the intermolecular interaction. He introduced two parameters, S and B, which are determining the band shape, S being the parameter related to the coupling between the electronic transition and the intramolecular vibration, and B being the one corresponding to the half-width of the exciton band. For a free molecule, the oscillator strength of the (0-n) vibronic band can be approximately given by Eq. 5.

† For the purpose to compare with the theoretical band shapes predicted by Sumi, we plotted here optical conductivity, not $\mathrm{Im}[\varepsilon(\omega)]$, against wave number. The optical conductivity was calculated from $\mathrm{Im}[\varepsilon(\omega)]$ by the following relation;

$$\sigma(\omega)=8.854\times10^{12}\omega\cdot\mathrm{Im}[\varepsilon(\omega)] \qquad [\Omega^{-1}\,cm^{-1}]$$

where $\mathrm{Im}[\varepsilon(\omega)]$ is expressed in c.g.s. units.

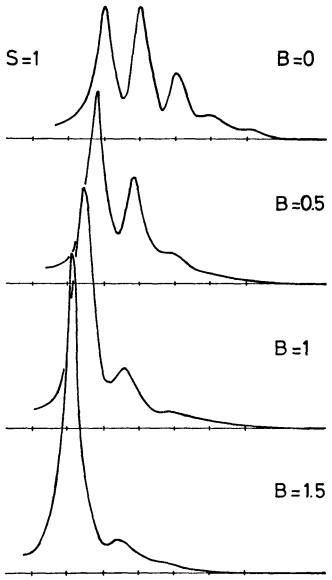

Fig. 7. Vibronic band shapes in optical conductivity spectra, theoretically predicted for various values of B, assuming that $S=1$. The spectra have been a little broadened than the original ones given in the paper by Sumi.[25]

$$f_{0-n} = A\frac{S^n}{n!}e^{-S} \tag{5}$$

When we apply the above relation to the $^2B_{1u}\leftarrow{}^2B_{2g}$ band of the solution spectrum of $TMPD^+$ ion, the S value is estimated to be 1.0 in the unit of a quantum of the intramolecular vibration.[26] Assuming that the same S value can be used for the corresponding LE band of WBP crystal, we compared the observed band shapes with the theoretical band shapes given by Sumi for different B values. The band shapes which are expected by Sumi's theory for the cases of $B=0$—1.5,[27] are illustrated in Fig. 7, where the width of each vibronic band has been a little broadened than the spectra given in Sumi's paper, for the purpose to compare with the observed spectra. When we compare the observed band shapes (Fig. 6) with the theoretical ones shown in Fig. 7, we can see that the observed band shape of the //b spectrum corresponds to the case of $B=0.5$—1.0 while that of the //a spectrum corresponds to the case of $B=0$—0.5.[27]

Since there are two sites of $TMPD^+$ in the unit cell, the exciton band associated with $^2B_{1u}$ molecular excited state splits into two bands, in which symmetries are B_{3u} and B_{2u}, respectively. The optical transition to B_{3u} exciton band is allowed for the a-axis polarized light, and that to B_{2u} exciton band is allowed for the b-axis polarized light. As shown in Table 1, the Davydov splitting of these two exciton states is about 400 cm^{-1}. The band shape analysis described above suggests that B_{2u} exciton band has a witdh of 1500—3000 cm^{-1} while B_{3u} exciton band has a considerably narrower band width, less than 1500 cm^{-1}.

Temperature Dependence of the Spectrum. WBP crystal undergoes a phase transition at about 190 K. The crystal of the low-temperature phase is monoclinic with the space group $B2_1/d$, the lattice constants being

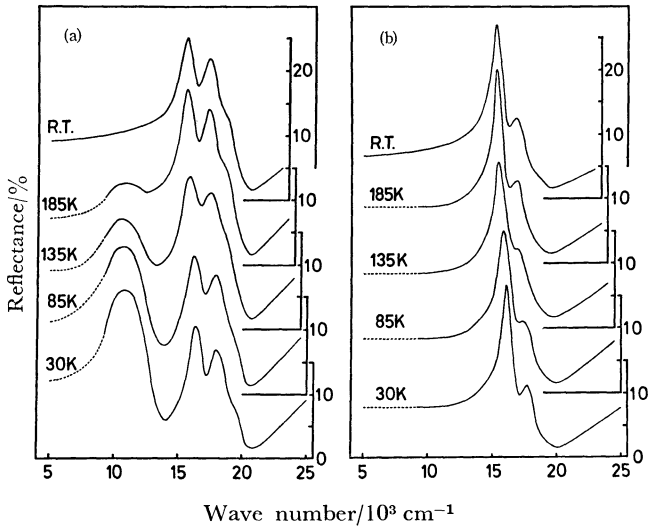

Fig. 8. Low-temperature reflection spectra of WBP. (a) //a spectra, (b) //b spectra.

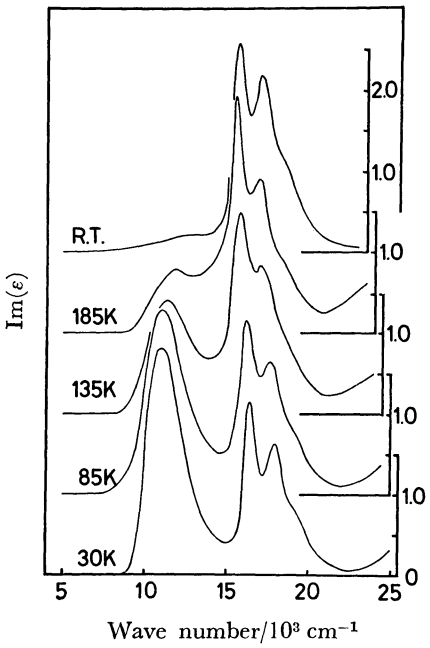

Fig. 9. Im[$\varepsilon(\omega)$] spectra (//a) obtained by the Kramers-Kronig transformation of the reflection spectra shown in Fig. 8.

$a=11.655$ Å, $b=10.147$ Å, $c=20.130$ Å, and $\beta=92.57°$ at 110 K.[11] As compared with the high-temperature phase, the lengths of the a- and b-axes are doubled in the low-temperature phase, and the unit cell contains eight molecular units of $TMPD^+\cdot ClO_4^-$. The $TMPD^+$ ions are stacked along the a-axis as in the high-temperature phase, but with an alternation of intermolecular spacing showing definitely the character of a dimeric arrangement. The reflection spectra measured for the //a and //b polarizations at various temperatures are shown in Fig. 8. It should be noted that, in the low-temperature phase, a new broad dispersion of reflectance appears in the region of 9×10^3—15×10^3 cm^{-1}, and its amplitude increases on lowering the temperature. This dispersion can be observed most

Table 2. Temperature dependence of the oscillator strength of the charge-transfer band and the triplet population estimated by various method

T/K	Oscillator strength		Triplet population/%			
			CT band		Paramagnetism[c]	Calcd by S-T model[d]
	K-K[a]	C-F[b]	K-K	C-F		
185	0.10	0.32	77	49	45	32
135	0.23	0.44	48	29	21	19
85	0.38	0.59	14	5	5	5
30	0.44	0.62	0	0	0	0

a) Kramers-Kronig transformation method. b) Curve-fitting (dispersion analysis) method. c) Estimated from the magnetic susceptibility data reported by Okumura.[2] d) Calculated by the singlet-triplet model, assuming the S-T separation as 235 cm^{-1}.[3]

strongly when the light is polarized parallel to the a-axis which is the direction of the $TMPD^+$ stack, and is not observable when the light is polarized perpendicular to it. This fact indicates that the dispersion mentioned above is associated with the charge transfer between $TMPD^+$ ions. Figure 9 shows the $Im[\varepsilon(\omega)]$ spectra obtained by Kramers-Kronig transformation of the //a reflection spectra. The general features of the obtained $Im[\varepsilon(\omega)]$ spectra are very similar to the low-temperature spectrum of WBP powder reported by Sakata and Nagakura.[10] The first absorption band is the charge-transfer band, which is very broad and structureless even at 30 K, having its absorption maximum at 11.6×10^3 cm^{-1}. Sakata and Nagakura pointed out that there is a close correlation between the decrease of the paramagnetic susceptibility and the increase of the intensity of the charge-transfer band.[8,10] Assuming the dimeric arrangement in $TMPD^+$ chain, they concluded that there is a thermally accessible triplet state (T_0) of $TMPD^+$ dimer above the ground singlet state (S_0), and since the optical transition to the charge-transfer (singlet) state of the dimer is allowed only from S_0, the decrease of the intensity of the CT band must be proportional to the increase of the triplet population, hence to the spin concentration. From the analysis of the temperature dependence of the CT band, they derived 230 ± 50 cm^{-1} for the singlet-triplet separation of the $TMPD^+$ dimer, which was in good agreement with the value (≈235 cm^{-1}) determined by Thomas *et al.*[3] from ESR data. We determined the oscillator strength of the CT band at each temperature from the observed spectrum, and estimated the fraction of $TMPD^+$ dimers which are in the triplet state, assuming that the transition moment of the CT transition does not vary with temperature. The results are given in Table 2. The triplet population $N_t(T)$ derived from the paramagnetic susceptibility χ_H by means of Eq. 6 and that calculated by the singlet-triplet model assuming the singlet-triplet separation of 235 cm^{-1}, are also given in the same table.

$$\chi_H = \frac{g^2\beta^2 S(S+1)}{3kT}\cdot N_t(T) \qquad (6)$$

As shown in Table 2, the results by Kramers-Kronig analysis and curve-fitting analysis are a little different from each other. Seemingly this disagreement arised

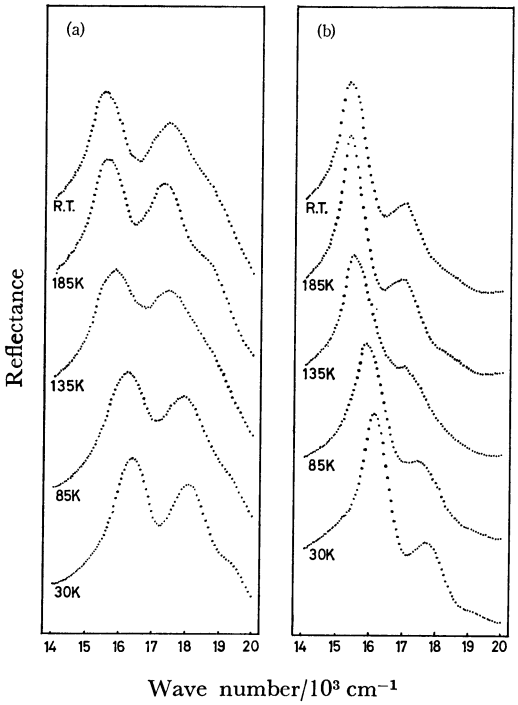

Fig. 10. Low-temperature reflection spectra, in the visible region, measured with 1.6 nm resolution.

from the inherent difficulty in determining the absolute value of oscillator strength from the reflectance data when an absorption band is very broad and weak as in the case of the CT band of WBP. No such discrepancy was found between the results of the two analysis methods in the case of the strong LE band of WBP crystal. The triplet population derived from the oscillator-strength values obtained by curve-fitting analysis, are in very good agreement with those derived from the paramagnetic susceptibility data. But this fact does not necessarily mean that the data by curve-fitting method are more reliable than those by Kramers-Kronig analysis, since the above agreement with the magnetic data looks too good if we take into account the situation that the transition moment of the CT excitation must vary to some extent with temperature accompanying the lattice contraction on lowering the temperature. Although there remains such a problem as regards the quantitative anaylsis of the

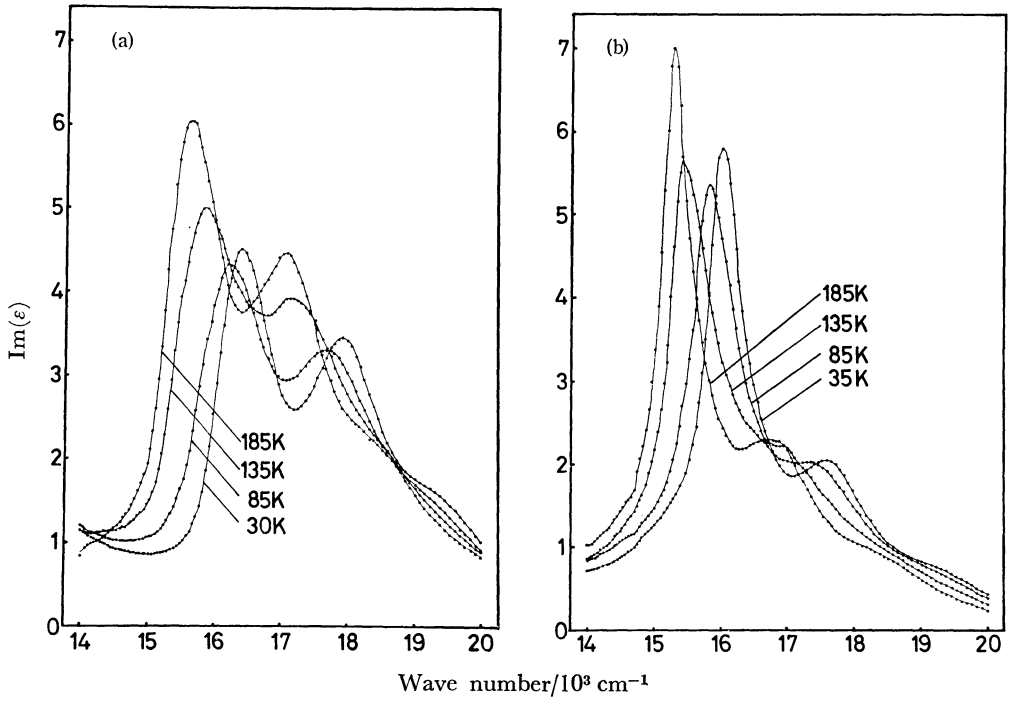

Fig. 11. Im[$\varepsilon(\omega)$] spectra obtained by the Kramers-Kronig transformation of the reflection spectra shown in Fig. 10: (a) //a spectra, (b) //b spectra.

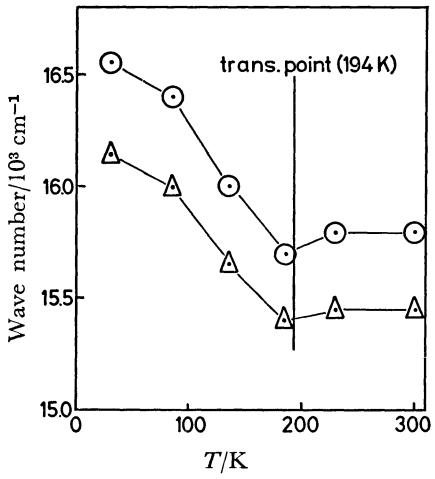

Fig. 12. Shift of the (0-0) band with temperature.

intensity change of the CT band, the results shown in Table 2 clearly indicate that the essential feature of the temperature dependence of the CT band can be well understood in terms of the singlet-triplet model as discussed by Sakata and Nagakura.[10] Incidentally, if we take up only the change, not the absolute value, of the oscillator strength with temperature, the results by the two analysis methods exactly agree with each other, and are also in good agreement with the data reported by Sakata and Nagakura for the spectrum of WBP powder.

The reflection spectrum in the region of 14×10^3—20×10^3 cm^{-1} was measured with an increased resolution, the resolution being 1.6 nm. The results are shown in Fig. 10. Figure 11 shows the Im[$\varepsilon(\omega)$] spectra obtained by Kramers-Kronig analysis of the above reflectance data. As we have mentioned in the case of the room-temperature spectrum, the absorption band appearing here is the LE band associated with the lowest π-π^* ($^2B_{1u}\leftarrow{}^2B_{2g}$) transition of TMPD$^+$. We can see three characteristic features of temperature dependence both in the //a spectrum and in the //b spectrum. The first is the shift of the absorption peaks with temperature. In Fig. 12, we plotted the wave number of the (0-0) band against temperature. One can clearly see that the position of the (0-0) band does not appreciably change with temperature in the high temperature phase, but is markedly blue-shifted on lowering the temperature in the low-temperature phase. The second is the change of the width of vibronic band. On lowering the temperature, the width gradually increases, shows the maximum broadness at 135 K, and then decreases at lower temperature. The third is the fact that the peak heights of the (0-0) and (0-1) bands gradually decrease on lowering the temperature from 185 K to 85 K and then increase at 30 K. In the case of a typical molecular crystal like anthracene, the (0-0) band shows a red-shift on lowering the temperature, the magnitude of this shift having been reported to be about 150 cm^{-1} between the room temperature and 4.2 K in the case of anthracene,[28] and usually the width of a vibronic band monotonously decreases on lowering the temperature. The temperature dependence observed for the LE band of WBP is very much different from the one mentioned above.

Examining the temperature dependence of the absorption spectrum of WBP powder, Sakata and Nagakura[10] reported that the spectra measured at different temperatures exhibited isosbestic points. They concluded that the singlet-singlet transition and the triplet-triplet transition of TMPD$^+$ dimer are overlapp-

ing on each other to give the observed LE band of the absorption spectrum of the powder, and the temperature dependence of its band shape can be understood by considering the thermal equilibrium between the singlet and triplet states of the dimer. The single-crystal spectra obtained in the present study show that the temperature dependence of the $\mathrm{Im}[\varepsilon(\omega)]$ spectrum of WBP crystal is, in reality, a little more complicated than described by the above authors. The observed spectra did not exhibit isosbestic points, so that it was not possible to carry out a simple quantitative analysis of the band shape in terms of the thermal equilibrium between the singlet and triplet states of $TMPD^+$ dimer. But the main feature of the observed temperature dependence can be understood, at least qualitatively, by the same model. As shown in Table 2, the triplet population becomes to be almost negligible at 30 K. Thus the band shape at 30 K can be regarded to be the one entirely due to the singlet-singlet transition, while, at higher temperatures, the band due to triplet-triplet transition is overlapping with the absorption band due to the singlet-singlet transition. Possibly, the band shape at just below the transition temperature is largely determined by the triplet-triplet absorption band. Seemingly this is the reason why the LE band is broader at intermediate temperatures. The shifts of absorption peaks and the change of the band shape suggest that the triplet-triplet absorption band is located at the wavenumber lower by 600—800 cm^{-1} than the singlet-singlet absorption band. We tried to reproduce the observed band shapes as the superposition of the singlet-singlet and triplet-triplet absorption bands, and found it necessary, in order to explain the observed band shapes, to consider that both the singlet-singlet and triplet-triplet absorption bands shift to higher wave number on lowering the temperature. This situation prevented us to carry out a further quantitative analysis of band shape, but we were able to conclude that the observed temperature dependence of the LE band is consistent with the change of the triplet population derived from the magnetic data or that from the intensity of the CT band.

The authors are grateful to Olympus Optical Co., Ltd. for their generous offer of the Olympus MMSP-RK system used in the present study. The authors wish to thank Dr. Koichi Ohno, Faculty of Education, The University of Tokyo, for helpful discussion.

References

1) W. Duffy, Jr., *J. Chem. Phys.*, **36**, 490 (1962).
2) K. Okumura, *J. Phys. Soc. Jpn.*, **18**, 69 (1963).
3) D. D. Thomas, H. Keller, and H. M. McConnell, *J. Chem. Phys.*, **39**, 2321 (1963).
4) H. J. Monkhorst and J. Kommandeur, *J. Chem. Phys.*, **47**, 391 (1967).
5) G. T. Pott and J. Kommandeur, *J. Chem. Phys.*, **47**, 395 (1967).
6) H. J. Monkhorst, G. T. Pott, and J. Kommandeur, *J. Chem. Phys.*, **47**, 401 (1967).
7) G. T. Pott, C. F. van Bruggen, and J. Kommandeur, *J. Chem. Phys.*, **47**, 408 (1967).
8) T. Sakata and S. Nagakura, *Bull. Chem. Soc. Jpn.*, **42**, 1499 (1969).
9) H. Chihara, M. Nakamura, and S. Seki, *Bull. Chem. Soc. Jpn.*, **38**, 1796 (1965).
10) T. Sakata and S. Nagakura, *Mol. Phys.*, **19**, 321 (1970).
11) J. L. de Boer and A. Vos, *Acta Crystallogr., Sect. B*, **28**, 835, 839 (1972).
12) Y. Iida, *Bull. Chem. Soc. Jpn.*, **41**, 2615 (1968).
13) J. Tanaka and M. Mizuno, *Bull. Chem. Soc. Jpn.*, **42**, 1841 (1969).
14) G. R. Anderson, *J. Chem. Phys.*, **47**, 3853 (1967).
15) K. Ishii, K. Kaneko, and H. Kuroda, *Bull. Chem. Soc. Jpn.*, **49**, 2077 (1976).
16) L. Michaelis and S. Granick, *J. Am. Chem. Soc.*, **65**, 1747 (1943).
17) K. Yakushi, M. Iguchi, and H. Kuroda, *Bull. Chem. Soc. Jpn.*, **52**, 3180 (1979).
18) The effect of aperture angle of objective lens was discussed in Ref. 17.
19) When the band exhibits a vibrational structure, we used one dispersion term for each vibronic band.
20) The resolution was 1.6 nm in these measurement.
21) R. K. Ahrenkiel, *J. Opt. Soc. Am.*, **61**, 1651 (1971).
22) Although the CT band appears with a considerable intensity the low-temperature spectrum of WBP crystal, it does not appear in the room-temperature spectrum.
23) In order to estimate those oriented-gas values of oscillator strength, we took three times of the observed oscillator sterngth of the corresponding absorption band of the solution spectrum.
24) J. S. Briggs and A. H. Herzenberg, *Mol. Phys.*, **21**, 865 (1971).
25) H. Sumi, *J. Phys. Soc. Jpn.*, **36**, 770 (1974); **38**, 825 (1975).
26) It is 1530 cm^{-1} in wave number.
27) The unit adopted here is the same as the one for the S value.
28) G. C. Morris and M. G. Sceats. *Chem. Phys.*, **3**, 164 (1974).